Development/Plasticity/Repair

Development of Thalamocortical Connectivity during Infancy and Its Cognitive Correlations

Sarael Alcauter,[1] Weili Lin,[1] J. Keith Smith,[2] Sarah J. Short,[3] Barbara D. Goldman,[4] J. Steven Reznick,[4] John H. Gilmore,[3] and Wei Gao[1]

[1]Department of Radiology and Biomedical Research Imaging Center, [2]Department of Radiology, [3]Department of Psychiatry, and [4]Frank Porter Graham Child Development Institute and Department of Psychology, University of North Carolina at Chapel Hill, Chapel Hill, North Carolina 27599

Although commonly viewed as a sensory information relay center, the thalamus has been increasingly recognized as an essential node in various higher-order cognitive circuits, and the underlying thalamocortical interaction mechanism has attracted increasing scientific interest. However, the development of thalamocortical connections and how such development relates to cognitive processes during the earliest stages of life remain largely unknown. Leveraging a large human pediatric sample ($N = 143$) with longitudinal resting-state fMRI scans and cognitive data collected during the first 2 years of life, we aimed to characterize the age-dependent development of thalamocortical connectivity patterns by examining the functional relationship between the thalamus and nine cortical functional networks and determine the correlation between thalamocortical connectivity and cognitive performance at ages 1 and 2 years. Our results revealed that the thalamus–sensorimotor and thalamus–salience connectivity networks were already present in neonates, whereas the thalamus–medial visual and thalamus–default mode network connectivity emerged later, at 1 year of age. More importantly, brain–behavior analyses based on the Mullen Early Learning Composite Score and visual–spatial working memory performance measured at 1 and 2 years of age highlighted significant correlations with the thalamus–salience network connectivity. These results provide new insights into the understudied early functional brain development process and shed light on the behavioral importance of the emerging thalamocortical connectivity during infancy.

Key words: **development; functional connectivity; Mullen scores; resting state; thalamus; working memory**

Introduction

Situated between the cerebral cortex and the midbrain, the thalamus is aptly located to serve as a relay center for peripheral sensory information to the cortex (Jones, 2007). However, recent evidence supports a more diverse role of the thalamus in higher-order cognitive functions (Jones, 2007; Sherman, 2007). Therefore, there is increasing interest in unveiling thalamocortical functional connectivity patterns in the adult population (Zhang et al., 2008; Kim et al., 2013). Delineating thalamocortical connectivity patterns in early development is also important because it has been suggested that the early establishment of appropriate thalamocortical connectivity is critical for the functional specialization of the cortex (Sharma et al., 2000; Jones, 2007) and disruptions of this process may be related to different developmental disorders such as schizophrenia (Marenco et al., 2012; Klingner et al., 2014), bipolar disorder (Anticevic et al., 2013), and autism (Nair et al., 2013). Nevertheless, despite one study comparing thalamocortical connectivity patterns between school-aged children and adults (Fair et al., 2010), there has not yet been a study investigating directly the earliest development of thalamocortical connectivity when the brain undergoes its most dynamic structural expansion (Gilmore et al., 2007; Knickmeyer et al., 2008; Gilmore et al., 2012) and functional evolution (Gao et al., 2009b; Tau and Peterson, 2010; Gao et al., 2011). There has also been no study characterizing the cognitive significance of thalamocortical connectivity during infancy.

Based on a large-scale longitudinal resting state fMRI (rs-fMRI) dataset ($N = 143$) covering the first 2 years of postnatal life and a novel network connectivity perspective, the primary aim of this study was to characterize the age-dependent thalamocortical connectivity patterns during infancy. Our secondary aim was to explore the cognitive significance of thalamocortical connectivity patterns by correlating them with children's Mullen Early Learning Composite Scores (Mullen, 1995) and visual–spatial working memory performance (Pelphrey and Reznick, 2003; Reznick, 2007) at ages 1 and 2 years. Previous studies have shown the early synchronization of different primary networks (Fransson et al., 2007; Lin et al., 2008; Doria et al., 2010) and the presence of the higher-order salience network at birth (Alcauter et al., 2013).

Received Feb. 26, 2014; revised May 27, 2014; accepted May 29, 2014.

Author contributions: S.A., W.L., J.H.G., and W.G. designed research; S.A., W.L., J.H.G., and W.G. performed research; S.A., and W.G. analyzed data; S.A., W.L., S.J.S., J.K.S., B.D.G., J.S.R., J.H.G., and W.G. wrote the paper.

This work was supported by the National Institutes of Health (Grant R01MH070890-09A1 to J.H.G.), the Foundation of Hope for Research and Treatment of Mental Illness (W.G.), and the University of North Carolina–Chapel Hill (Start-up Grant to W.G.). We thank the many research assistants (in chronological order) who conducted the Mullen and working memory assessments for this study: Hillary Langley, Sarah Palmer, Portia Henderson, Molly McGinnis, Emily Bostwick, Sadie Hasbrouck, Monica Ferenz, Kassidy Jezierski, Haley Parrish, and Margot Williams.

The authors declare no competing financial interests.

Correspondence should be addressed to Wei Gao, PhD, University of North Carolina at Chapel Hill, Department of Radiology and Biomedical Research Imaging Center, Rm 3105, Bioinformatics Building, Chapel Hill, NC 27599. E-mail: wgao@email.unc.edu.

DOI:10.1523/JNEUROSCI.0796-14.2014

 0270-6474/14/349067-09$15.00/0

Table 1. Demographic information of the participants included in this study

Age at scans (year)	Singletons	Twins	Total
0 and 1	26 (10 male)	25 (15 male)	51 (25 male)
0 and 2	4 (3 male)	10 (4 male)	14 (7 male)
1 and 2	15 (11 male)	16 (10 male)	31 (21 male)
0, 1, and 2	20 (11 male)	27 (13 male)	47 (24 male)
Total	65 (35 male)	78 (42 male)	143 (77 male)

Given the importance of thalamic input for the proper functioning of these networks (Seeley et al., 2007; Guldenmund et al., 2013), we hypothesized the emergence of thalamus–primary and thalamus–salience connectivity in neonates. However, considering the dramatic postnatal functional development (Gao et al., 2009a; Gao et al., 2009b; Gao et al., 2013b), we also expected significant reorganization of neonatal connectivity patterns and the emergence of additional thalamocortical connections at 1 and 2 years of age. Finally, we hypothesized significant correlations between the strength of thalamocortical connectivity and cognitive performance. In particular, based on the early emergence of the salience network (Alcauter et al., 2013) and its versatile functional roles supporting working memory and general cognition (Seeley et al., 2007; Smith et al., 2009; Menon and Uddin, 2010), we hypothesized that the thalamus–salience connectivity would be particularly important for brain–behavioral relationships. Our results confirmed most of our hypotheses and revealed new insights into early thalamocortical connectivity development.

Materials and Methods

Subjects. Participants were part of a large study characterizing brain development in healthy and high-risk children (Gao et al., 2009b; Gilmore et al., 2012; Alcauter et al., 2013; Short et al., 2013). We retrospectively identified 143 healthy subjects (77 males) scanned at least twice during the first 2 years of life: neonates ($n = 112$, mean age $= 33 \pm 19$ d), 1-year-olds ($n = 129$, mean age $= 397 \pm 35$ d), and 2-year-olds ($n = 92$, mean age $= 762 \pm 33$ d). Among the participants, 65 were healthy singleton subjects (35 males; 50 neonate scans, mean age $= 23 \pm 9$ d; 61 1-year-old scans, mean age $= 380 \pm 21$ d; 39 2-year-old scans, mean age $= 745 \pm 27$ d) and 78 were from healthy twin subjects (only 1 of each twin pair was included; 42 males; 62 neonate scans, mean age $= 40 \pm 21$ d; 68 1-year-old scans, mean age $= 412 \pm 38$ d; 53 2-year-old scans, mean age $= 774 \pm 31$ d).

The distribution of ages at which the participants were scanned is shown in Table 1. Inclusion criteria included birth between 35 and 42 weeks gestational age, appropriate weight for the gestational age, and the absence of major pregnancy and delivery complications, as defined in the following exclusion criteria. Exclusion criteria included maternal preeclampsia, placental abruption, neonatal hypoxia, any neonatal illness requiring greater than a 1 d stay in the neonatal intensive care unit, mother with HIV, mother with any psychiatric disorder, mother using illegal drugs/narcotics during pregnancy, and any chromosomal or major congenital abnormality. Informed written consent was obtained from the parents of all infant participants and all study protocols were approved by the University of North Carolina at Chapel Hill's Institutional Review Board. Before imaging, subjects were fed, swaddled, and fitted with ear protection. All subjects were in a natural sleep during the imaging session. A board-certified neuroradiologist (J.K.S.) reviewed all images to verify that there were no significant abnormalities.

Imaging. The majority of images were acquired with a 3T Allegra head-only MR scanner (Siemens) using a circular polarization head coil. A small number of images (1 neonate, 11 1-year-olds, and 14 2-year-olds) were acquired with a 3T Trio MR scanner (Siemens) using a 32-channel head coil. rsfMRI images were acquired using a T2*-weighted EPI sequence with identical parameters from the 2 scanners: TR = 2 s, TE = 32 ms, 33 slices, voxel size of $4 \times 4 \times 4$ mm^3. A total of 150 volumes were acquired in a 5 min scan. Our *post hoc* analyses of functional connectivity within major cortical functional networks and the thalamocortical connectivity (detailed in the following section) did not reveal any significant differences between the data from the two scanners, so all data were pooled together for subsequent analyses. To provide anatomical reference, structural images were acquired using a 3D MP-RAGE sequence (Allegra scanner: TR = 1820 ms, TE = 4.38 ms, inversion time = 1100 ms; Trio scanner: TR = 1900 ms, TE = 3.74 ms, inversion time = 1100 ms) with a voxel size of $1 \times 1 \times 1$ mm^3.

Data preprocessing. Functional data were preprocessed using FMRIB's Software Libraries (FSL, version 4.1.9; Smith et al., 2004; Jenkinson et al., 2012). The preprocessing steps included discarding the first 10 volumes, slice-timing correction, motion correction, and band-pass filtering (0.01–0.08 Hz). Mean signal from white matter, CSF, and six motion parameters were removed using linear regression. No spatial smoothing was applied. To further reduce the effect of motion on functional connectivity measures, the global measure of signal change and framewise displacement (FD) were controlled to be <0.5% signal and 0.5 mm, respectively, as proposed by Power et al. (2012). A lower limit of >90 volumes remained after this "scrubbing" process was set as one of the inclusion criteria. Detailed information about the volumes removed for each subject and residual FD measures may be found in Gao et al. (2014b). The residual FD after the "scrubbing" process was included as a covariate of no interest in all subsequent statistical modeling and behavioral correlations to control for residual motion artifacts. For each subject and session, after an initial rigid alignment between functional data and T1-weighted high-resolution structural images, a nonlinear transformation field was obtained with FSL's fnirt (Smith et al., 2004; Jenkinson et al., 2012) from individual T1-weighted images to a longitudinal T1 template; that is, T1-weighted images of a subject scanned at 2 weeks, 1 year, and 2 years. A combined transformation field was used to warp the preprocessed rsfMRI data to the longitudinal template. In addition, nonlinear transformation fields were obtained from the longitudinal template to the Montreal Neurological Institute (MNI) standard space using a 4D registration method, 4D-HAMMER (Shen and Davatzikos, 2004), which significantly improves warping accuracy over a series of independent 3D warping. All further postprocessing was done in the longitudinal age-specific template space and the common MNI representations were used for visualization purposes.

Functional networks definition. To explore the cortical projections of the thalamus, we selected nine well recognized cortical networks described previously (Smith et al., 2009). Specifically, the medial visual, occipital poles, lateral visual, default mode, sensorimotor, auditory, salience, and left and right frontoparietal networks were included. Seed regions were defined as 8-mm-radius spheres centered in the local maxima of each network's statistical map provided by Smith et al. (2009)- and warped to the longitudinal age-specific templates to obtain seed-based connectivity maps using partial correlation (controlling for the other eight seeds). After Fisher's z transformation, one-sample t tests were performed to obtain group-level significant connectivity maps. Significance was defined as $p < 0.05$ after false discovery rate (FDR) correction (Benjamini and Yekutieli, 2001). To define specific thalamus clusters that project to one of the nine networks, nonoverlapping network cortical masks were derived using a functional connectivity threshold of 0.1 (consistently more stringent than the threshold of FDR-corrected $p < 0.05$), together with a "winner-takes-all" approach (Zhang et al., 2008; Buckner et al., 2011; Yeo et al., 2011), to eliminate potential overlapping between different network masks. All cortical networks were constrained within a cortical mask based on the Harvard-Oxford cortical atlas (Frazier et al., 2005; Desikan et al., 2006; Jenkinson et al., 2012).

Thalamus definition and functional segmentation. The thalamus was defined based on the Harvard-Oxford probabilistic subcortical atlas provided with FSL (version 4.1.9) using a probability threshold of 50% and warped to the age-specific longitudinal template space, resulting in a thalamus mask for each age group (77, 173, and 206 voxels for neonate, 1-year-olds, and 2-year-olds, respectively). For each subject, the average time series derived from averaging within the cortical mask of each functional network was correlated with each thalamus voxel time series. Partial correlations controlling for the time series from the other cortical networks were used in the analysis to characterize specific thalamocorti-

Table 2. Consistency of thalamus parcellation

Age	Singletons, twins	Singletons, whole sample	Twins, whole sample	Pooled sample* (average ± SD)
Neonate	74%	88%	82%	79 ± 5%
1 y	86%	92%	92%	87 ± 3%
2 y	84%	91%	91%	80 ± 4%

*Based on 100 random subdivisions of the pooled sample into two subsamples.

cal connectivity. Adopting a winner-takes-all approach (Zhang et al., 2008; Buckner et al., 2011; Yeo et al., 2011), each thalamus voxel was labeled according to the cortical network with which it demonstrated the strongest group-level mean partial correlation. The thalamic parcellation maps from singletons and twin subjects were evaluated separately to test their similarity. Consistency was calculated as the percentage of voxels that showed the same network labeling between singleton and twin samples over the total number of voxels within the thalamus. Given the high level of consistency between singletons and twins (Table 2), they were merged to form one large sample. The consistency of thalamocortical projection was further evaluated using both a random subdivision approach and a bootstrapping strategy. For the random subdivision approach, the data within each age group were randomly divided into two independent samples and the consistency was evaluated between the two samples similarly as described in this section. This process was repeated 100 times to estimate the mean and standard deviation (SD) of the parcellation consistency. Finally, for the bootstrapping strategy, 10,000 random samplings with replacement were conducted for each age group and the corresponding group-level thalamocortical projection maps were obtained. Consistency of each voxel's labeling was calculated as the percentage of the most-frequent network label over 10,000.

Given that the winner-takes-all approach may potentially mask secondary but significant connections (Zhang et al., 2008; Buckner et al., 2011; Yeo et al., 2011), the cortical projection map of each defined thalamus cluster was reconstructed and examined. Specifically, the partial correlation was calculated between the average time series from each thalamic cluster and all other voxels of the cortex after controlling for the average time series from the other thalamic clusters. After a Fisher's z transformation, one-sample t tests were performed to obtain group-level significant connectivity maps. Significance was defined as $p < 0.05$ after FDR correction (Benjamini and Yekutieli, 2001).

Longitudinal network analysis. To characterize the longitudinal development of thalamocortical connections, regions of interest (ROIs) were defined based on the data from the 2-year-olds. Specifically, the spatial regions involved in each nonoverlapping cortical functional network were identified in the 2-year-old group using a clustering algorithm (Smith et al., 2004; Jenkinson et al., 2012) with the intensity threshold set to 0.1, 6-face connectivity, and a minimum cluster size of 15 voxels ($\sim$ 1000 mm^3). Subsequently, the defined thalamic clusters and cortical network ROIs in 2-year-olds were warped to the neonates and 1-year-olds so that a consistent set of ROIs were used for delineating the longitudinal growth curves. For each subject, a partial correlation matrix of all regions (i.e., including both thalamic clusters and cortical network ROIs) was calculated. After Fisher's z transformation, the significant positive connections were identified with a single-group t test (significant at $p < 0.05$, FDR corrected). Based on the individual correlation matrices, the mean connectivity between all thalamic clusters and the corresponding cortical projection regions with significant connectivity at the group level was calculated for each subject to represent the overall thalamocortical network connectivity, which was subsequently modeled using linear mixed-effect regression models (Verbeke and Molenberghs, 2009). Both a linear model and a log-linear model were built with thalamocortical functional connectivity measures as dependent variables and age or log(age) as fixed-effect independent variables. Random effects were added for the intercept and the age or log(age) terms. The singleton/twin information and the residual FD after the "scrubbing" process were included as covariates of no interest to control for possible singleton/twin differences and residual motion effects. Significance was defined as $p < 0.05$ and the Akaike information criterion was used to determine whether the linear or log-linear model with age was a better fit for the data.

Cognitive performance correlation. Participants were assessed using the Mullen Scales of Early Learning (Mullen, 1995) and a visual–spatial working memory test (Reznick, 2009) at 1 year (mean = 12.29 ± 0.64, range = 11–15 months) and 2 years (mean = 24.33 ± 0.83, range = 22–28 months) of adjusted age. The working memory assessment at 1 year was described previously (Short et al., 2013). Details are provided about both measurements at age 1 and age 2 in the following sections.

The performance on the four cognitive Mullen scales (visual reception, fine motor, receptive language, and expressive language) are combined to create the cognitive composite, the Mullen Early Learning Composite Standard Score (ELCSS), which ranges from 50 to 150, with a mean of 100 and a SD of 15, similar to other overall tests of cognitive development commonly referred to as IQ.

At both age 1 and age 2, the working memory assessment consisted of a set of trials of laboratory-developed hiding games that had been developed as part of a separate behavioral research program (Pelphrey and Reznick, 2003; Pelphrey et al., 2004; Reznick et al., 2004; Reznick, 2007, 2009) for which scores were calculated as the percentage of searches in the correct location. We have previously reported research on working memory performance at 10 and 12 months and nutritional supplementation (Cheatham et al., 2012) and documented relationships between working memory performance at 1 year and white matter microstructure (Short et al., 2013). Specifically, at age 1, after determining which of several small toys seemed the most interesting, the infant, sitting in the parent's lap, was familiarized with the hiding apparatus and allowed to first retrieve toys in plain sight in two locations and then to retrieve toys hidden under a felt cloth. Up to 12 hide-and-find trials were then administered; there were two hiding wells for the first six trials, and three hiding wells for the last six trials. Delays of 3, 9, and 15 s between the time of hiding and when the infant was allowed to search were distributed across each set of 6 trials. One-year-olds played one 12-trial game near the beginning of their testing session and one near the end of the session; the "best" percent correct score was selected from the 2 administrations that included at least 8 of the 12 possible trials. At age 2, the procedure was similar, except that the 2 working memory administrations included 10 trials and were slightly different in format, but both included 5 trials with 3 hiding places and 5 trials with 5 hiding places. Delays were 7, 14, and 21 s, distributed across the session. Again, best performance (percent of correct trials) on the games that included at least 7 of the 10 trials was used for analysis. For both ages, the hiding locations of the toys were counterbalanced.

The relationship between thalamocortical connectivity strength and cognitive data (i.e., the Mullen ELCSS scores and the percentages of correct trials for the working memory assessment) was explored in terms of Pearson's partial correlations, controlling for singleton/twin labels and residual FD information. The age-specific (1-year-old and 2-year-old) correlations were explored based on the thalamocortical network connectivity measured using age-specific ROIs, whereas the predictions (i.e., early functional connectivity data predicting later cognitive performance) were based on the connectivity matrices derived using the common ROIs defined in the 2-year-old group (see Longitudinal Network Analysis section). Significance was defined as $p < 0.05$ after FDR correction. To validate our findings, bootstrapping of the observed correlations was performed based on 10,000 times resampling with replacement and the 95% bootstrap confidence interval was calculated for each identified correlation.

Results

The functional connectivity maps of the 9 functional networks used as anchoring points to delineate specific thalamic clusters during the first 2 years of postnatal life are presented in Figure 1. Highly consistent with our previous results (Gao et al., 2014a; Gao et al., 2014b), primary networks including sensorimotor, auditory, medial visual, and occipital pole networks showed adult-like connectivity patterns in neonates. The salience network in neonates diffusively covered most key structures observed in adults (i.e., bilateral anterior insula, anterior cingulate cortex, and bilateral prefrontal cortex; Seeley et al., 2007; Alcauter et al., 2013), but local specialization was observed during the postnatal development. Other higher-order networks, including lateral visual, default mode, and bilateral frontoparietal

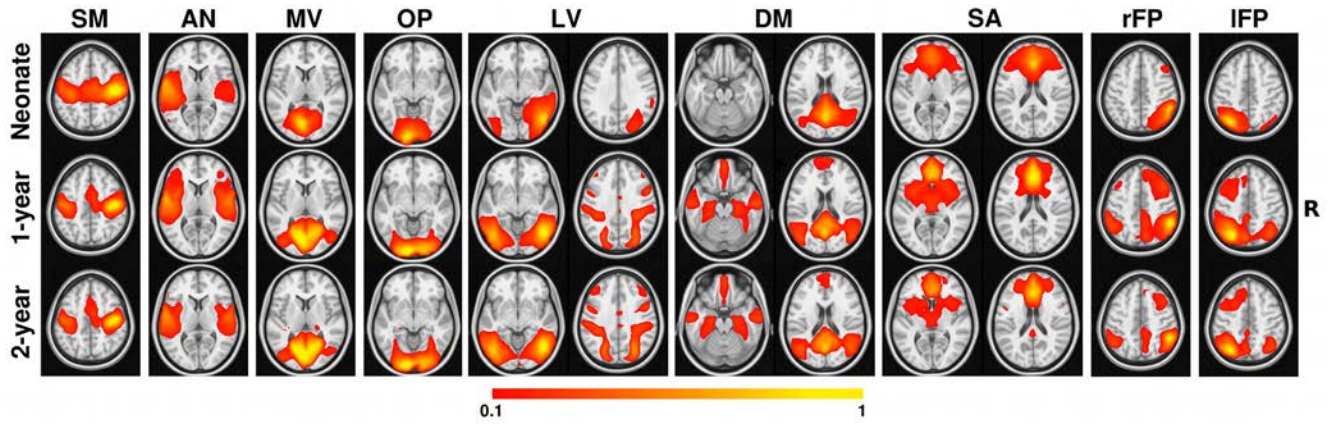

Figure 1. Development of the nine cortical functional networks. Color bar denotes correlation strength. The right side of the brain is in the right side of the image. SM, Sensorimotor; AN, auditory; MV, medial visual; OP, occipital poles; LV, lateral visual; DM, default mode; SA, salience; rFP/lFP, right/left frontoparietal.

networks, demonstrated dramatic improvements in their corresponding network topography from isolated local regions to distributed network structures during the first year, which continued to strengthen during the second year. Particularly, in 1-year-olds, the lateral visual network connectivity dramatically increased within the parietal and prefrontal regions and the default mode network extended to cover distant clusters within the medial prefrontal cortex (mPFC), superior frontal gyri, lateral middle temporal cortex, hippocampal formation areas, and lateral temporal-parietal areas, making both networks almost adult-like at this age. The bilateral frontoparietal networks also showed dramatic synchronization with ipsilateral dorsal prefrontal and contralateral superior parietal regions at 1 year of age. Overall, for all higher-order networks, a nonlinear developmental pattern was observed, with the most dramatic synchronization taking place during the first year, followed by minor refinement during the second year.

By calculating the partial correlation between thalamus voxels and different cortical networks, each thalamus voxel was labeled to the network with which it showed the strongest connectivity (i.e., winner-takes-all). Based on this strategy, the thalamic parcellation patterns were highly consistent between singletons and twins (Table 2), so they were merged to form one large sample to derive a general thalamocortical connectivity pattern (Alcauter et al., 2013).

The consistency of thalamocortical connectivity patterns within the pooled sample based on the random division approach is listed in Table 2. The mean and SD of the consistency of thalamic functional parcellation across the 100-times randomly divided subsamples were 79 ± 5%, 87 ± 3%, and 80 ± 4% for neonates, 1-year-olds, and 2-year-olds, respectively. The bootstrapping results are visualized in Figure 2*A*. Again, a generally high level of consistency was observed for all three age groups; overall, 71%, 88%, and 80% of voxels demonstrated >80% consistency in labeling for the neonates, 1-year olds, and 2-year-olds, respectively (Fig. 2*B*). Relatively low consistency was observed mainly within the boundary areas of the thalamus (Fig. 2*A*).

The thalamus parcellation topography within voxels showing >80% consistency in their cortical network labeling are presented in Figure 3*A*. Generally, bilateral symmetric thalamic clusters were observed for all three age groups. Specifically, in neonates, the functional parcellation revealed two thalamic clusters connecting to the sensorimotor and salience networks, respectively. The large sensorimotor cluster covered the central part of the thalamus spanning across the ventral-dorsal dimension, most likely including portions of the ventral nuclear group, but extending to the anterior, medial dorsal, and pulvinar nuclei (Niemann et al., 2000; Jones, 2007). In contrast, the salience network cluster was limited to the most anterior portion of the thalamus, resembling part of the ventral anterior nucleus (Niemann et al., 2000; Jones, 2007). In 1-year-olds, the sensorimotor cluster dramatically shrank to the ventral/lateral regions, resembling the ventral-lateral, ventral-posterolateral, and ventral-posteromedial nuclei locations, whereas the salience cluster expanded to cover the anterior and dorsal portion of the thalamus, resembling the anterior and medial dorsal nuclei (Niemann et al., 2000; Jones, 2007). More importantly, new thalamic clusters were identified for the medial visual and default mode networks at this age. Specifically, the newly emerged medial visual cluster mainly resided in the posterior lateral part of the thalamus, resembling the lateral geniculate bodies and lateral pulvinar, whereas the default mode cluster was restricted to the central posterior thalamus, part of the pulvinar nucleus (Niemann et al., 2000; Jones, 2007). The thalamic parcellation scheme in 2-year-olds remained highly consistent with that in 1-year-olds (Fig. 3*A*).

The reconstructed cortical projection structures of all identified thalamic clusters are visualized in Figure 3*B*. Generally, highly specific cortical projections for all thalamic clusters were observed, with the exception of the sensorimotor cluster in neonates, which projected not only to typical sensorimotor regions, but also to medial occipital and auditory areas. The neonatal salience cluster was primarily connected with the anterior frontal and insula regions that typically belong to the adult salience network (Seeley et al., 2007). In 1-year-olds, the cortical connectivity patterns were more specific and network-like than those of the neonates: the sensorimotor cluster projected to bilateral sensorimotor and supplementary motor regions; the salience cluster was connected to the anterior cingulate cortex, anterior insula, and regions of the PFC; the newly emerged medial visual cluster showed specific projections to medial occipital regions; and the default mode cluster synchronized with distributed regions in the posterior cingulate cortex, bilateral hippocampus formation areas, and regions of the mPFC. The cortical connectivity structures of 2-year-olds remained highly consistent with those of 1-year-olds, although there were noticeable expansions of the default mode cluster projections to bilateral inferior parietal lobule areas and inferior temporal cortices, as well as certain refinements of sensorimotor and salience cluster projections.

Significant log-linear growth of thalamocortical connections were observed when assessing the overall thalamocortical projections (Fig. 4*A*). For behavioral correlations, 1-year-old thalamus–

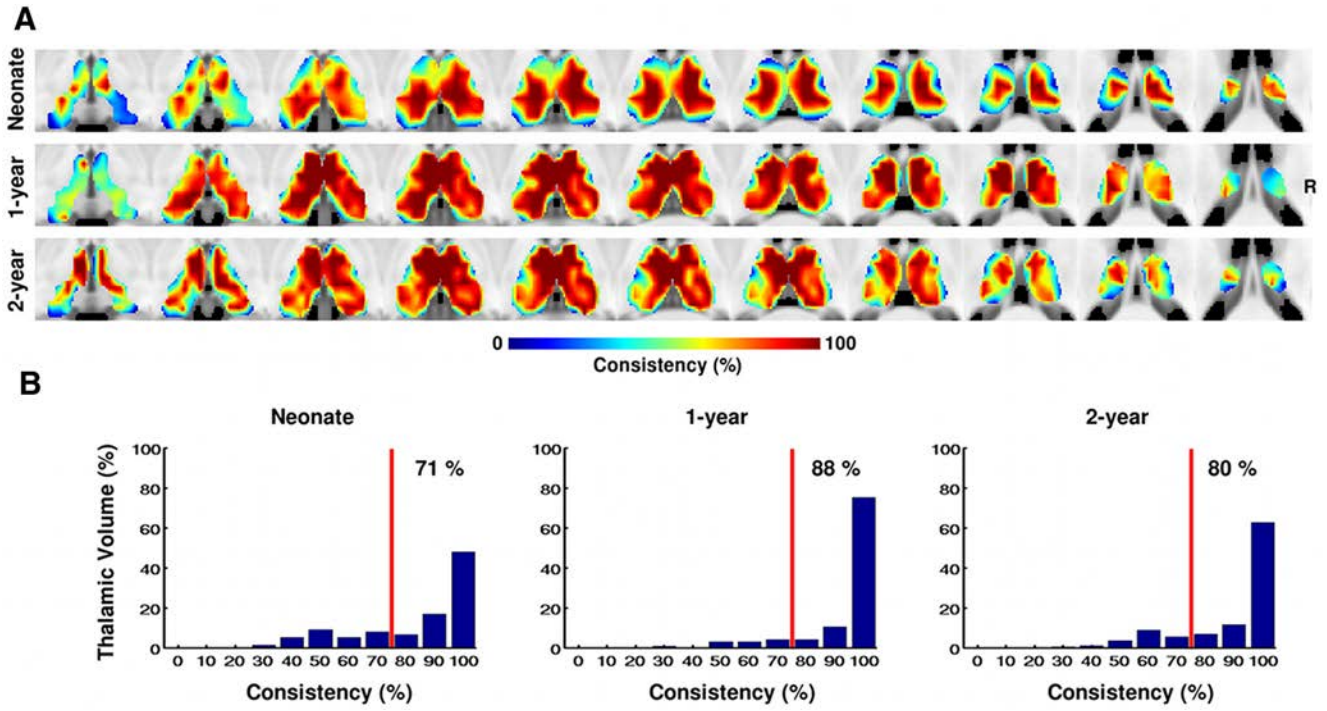

Figure 2. Consistency of the thalamic parcellation based on its cortical network projections within the whole sample. ***A***, Consistency maps across bootstrapped samples ($n = 10{,}000$) for all three age groups. The right side of the brain is on the right side of the image. ***B***, Corresponding histograms of the consistency values for the three age groups. Red vertical lines indicate 80% consistency level. The number shown in each plot indicates the percentage of thalamic voxels with a consistency level >80%.

salience network connectivity significantly predicted working memory performance in 2-year-olds ($r = 0.3525$, $p = 0.0024$, bootstrapping confidence interval: [0.0557, 0.5523]; Fig. 4*B*). Although not surviving multiple corrections, 1-year-old thalamus–salience network connectivity also predicted 2-year-old Mullen ELCSS with marginal significance ($r = 0.2645$, $p = 0.0113$, bootstrapping confidence interval: [0.0825, 0.3930]; Fig. 4*C*). Finally, the 1-year-old thalamus–salience connectivity also showed a trend of correlation with working memory performance measured at the same age ($r = 0.2020$, $p = 0.0671$, bootstrapping confidence interval: [−0.0649, 0.4201]). No statistical significance was detected for any other thalamocortical connections.

Discussion

In this study, we delineated the development of thalamocortical connectivity patterns during the first 2 postnatal years and their behavioral correlations. In particular, thalamus–sensorimotor and thalamus–salience network connectivity already exists in neonates, and new thalamus–medial–visual and thalamus–default mode network connectivity emerges in 1-year-olds and 2-year-olds. In addition, the brain–behavior analyses showed significant predictions centered on the thalamus–salience network connectivity. To our knowledge, this is the first set of results showing directly a relationship between infant brain functional connectivity and cognitive performance, which highlights the importance of thalamus–salience network connectivity in early cognitive development.

Thalamus cluster connecting with primary functional networks during infancy

The sensorimotor network showed robust connectivity with ventrolateral thalamus across the first 2 years (Fig. 3). In 1-year-olds and 2-year-olds, these regions resemble the location of ventral-lateral, ventral-posterolateral, and ventral-posteromedial nuclei (Niemann et al., 2000; Jones, 2007) and seem to overlap with the sensory/motor thalamic clusters identified in older populations (Behrens et al., 2003; Zhang et al., 2008; Fair et al., 2010; Zhang et al., 2010). This finding is not surprising given the critical importance of thalamus-relayed sensory inputs for the proper functioning of sensorimotor functions essential for early survival. This finding is also consistent with the establishment of structural thalamus-sensory pathways (Rakic and Goldman-Rakic, 1982; Kostovic and Goldman-Rakic, 1983; Kostovic and Rakic, 1984), the early synchronization of the sensorimotor network (Lin et al., 2008; Doria et al., 2011), and its functional responses observed at birth (Bartocci et al., 2006; Shibata et al., 2012).

A retrospective examination of the thalamic sensorimotor cluster cortical projections (Fig. 3*B*), however, also revealed multimodal covering of visual and auditory areas. This finding may reflect a low level of functional specialization within the thalamus at this early age. Anatomically, it has been shown in newborn rodents that neurons from motor and visual cortices project to common targets in the brainstem and spinal cord (O'Leary and Koester, 1993; Luo and O'Leary, 2005), but modality-specific projections develop during postnatal development after activity-dependent axonal pruning (Stanfield et al., 1982; O'Leary and Koester, 1993). Therefore, the seemingly diffusive thalamic sensorimotor cluster and the multimodal thalamocortical projections observed in neonates may become functionally specialized at a later age (Fig. 3). Indeed, the sensorimotor cluster dramatically shrank starting from 1 year of age, and 2 spatially nonoverlapping thalamic clusters emerged and projected to specific medial visual and sensorimotor regions, respectively, providing evidence for the low-level-specialization hypothesis. Conversely, this interesting finding might indicate that the thalamus may act as an "information exchanging hub" between the three sensory modalities to facilitate information integration and integrative development. This notion is consistent

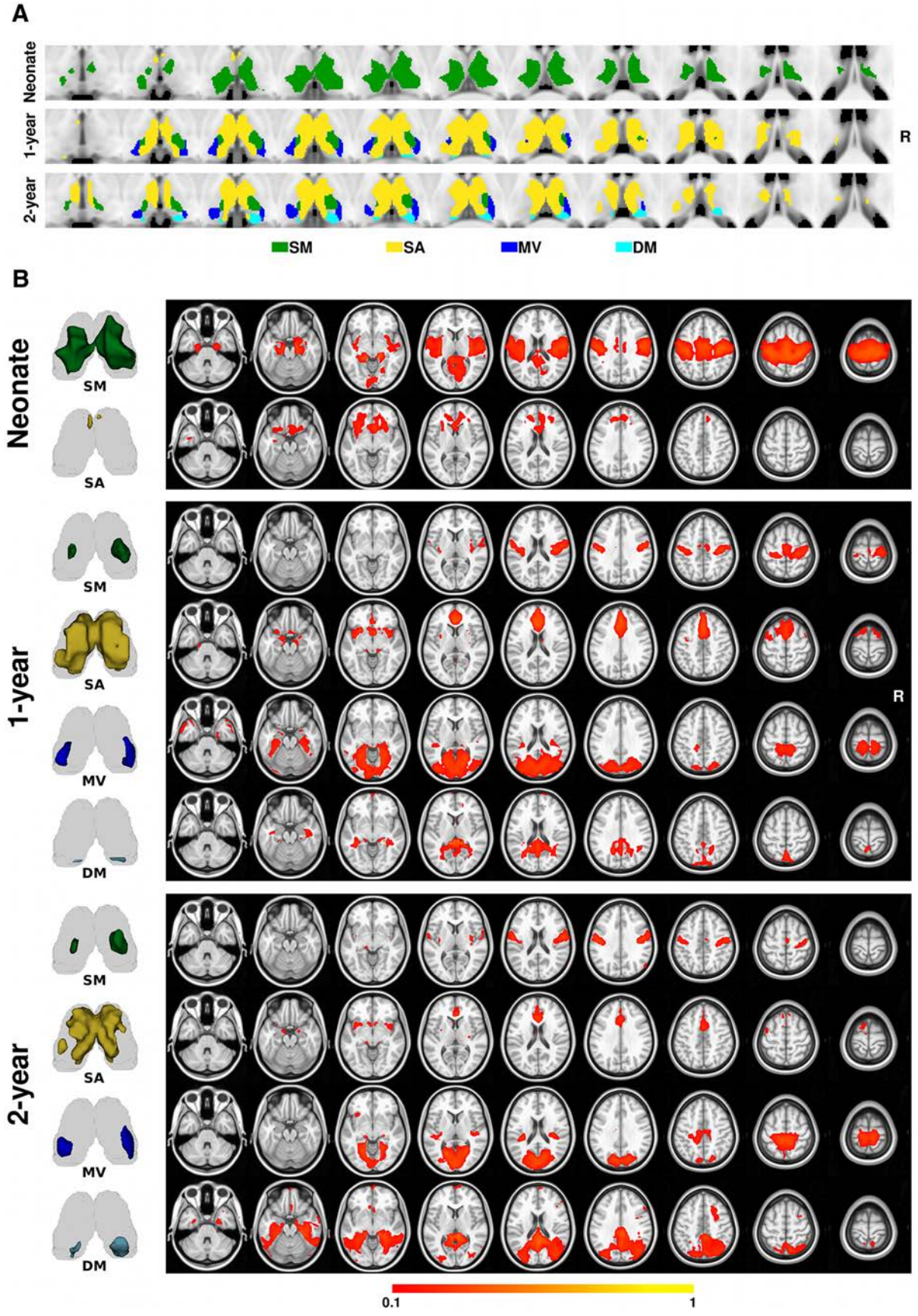

Figure 3. Thalamus parcellation and thalamocortical projection patterns for all three age groups. ***A***, Thalamus parcellation scheme based on the pooled large sample. ***B***, Cortical connectivity patterns associated with each thalamic cluster in ***A***. The 3D rendering of each thalamic cluster is visualized alongside its cortical projection map for easier interpretation. Color bar denotes connectivity strength. The right side of the brain is on the right side of the image. SM, Sensorimotor; SA, salience; DM, default mode; MV, medial visual.

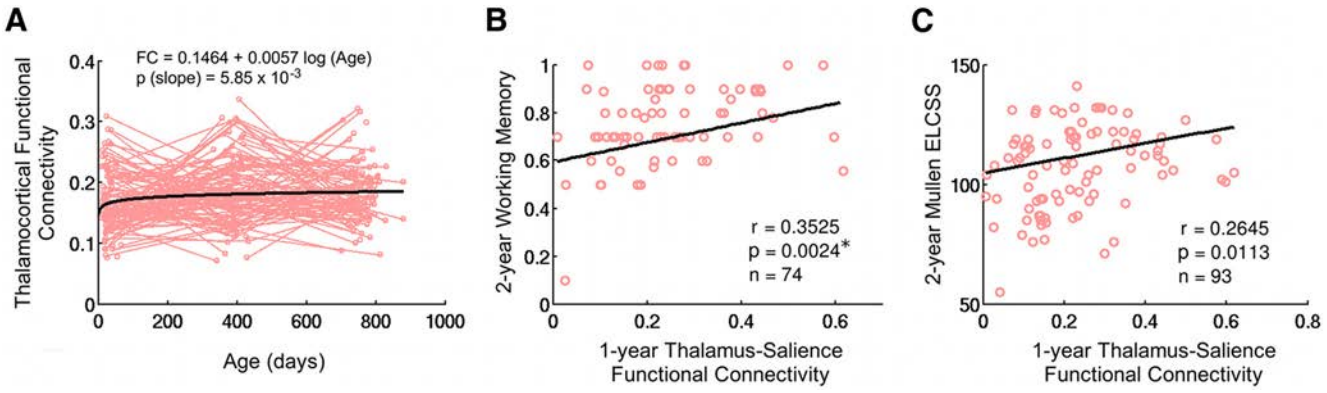

Figure 4. Thalamocortical connectivity growth and its correlation with cognitive scores. ***A***, Longitudinal growth of thalamocortical connectivity. Light red lines denote individual growth trajectories and the bold black line represents the log-linear fit of the growth trends (significant growth at $p < 0.05$). ***B***, Relationship between thalamus–salience network connectivity in 1-year-olds and working memory score in 2-year-olds. ***C***, Relationship between thalamus–salience network connectivity in 1-year-olds and Mullen ELCSS in 2-year-olds. *Significant after FDR correction, controlling for three prediction levels and four networks.

with the observation of a "mirror neuron system (MNS)" in adults that fires both when subjects perform and when they hear or observe others perform certain actions (Iacoboni et al., 1999). Although the adult MNS may rely mainly on higher-order frontal and parietal regions (Iacoboni et al., 1999), the prototype version of such functions might use subcortical mediations, as indicated in this study, for better integrated development during infancy. More studies are needed to tease apart these two hypotheses with differential developmental implications.

Thalamus cluster connecting with the salience network during infancy

Consistent with the significant involvement of thalamus in the adult salience network (Seeley et al., 2007) and the early emergence of this network (Alcauter et al., 2013), we observed thalamus–salience network connectivity in the neonates in the present study. In contrast to the multimodal projection pattern of the sensorimotor cluster, the cortical projections of the salience cluster concentrate on typical salience network regions (i.e., bilateral anterior insula, anterior cingulate, and prefrontal regions; Seeley et al., 2007) across different age groups, although the projection topography becomes more network-like as infants develop (Fig. 3). Consistent with our findings, the anterior insula, orbitofrontal cortex, amygdala, and thalamus were reported to be collectively active in newborns exposed to milk odors (Arichi et al., 2013), recognized as a trigger to orient the subjects toward their mother's breast (Varendi and Porter, 2001). Therefore, the observed thalamus–salience network connectivity in neonates may partly underlie this critical capability of food/security localization (Porter and Winberg, 1999; Arichi et al., 2013).

Importantly, our analyses of the relationship between thalamocortical connectivity and cognitive performance highlights the thalamus–salience connectivity as the only significant predictor for working memory performance and general intellectual development, further underscoring the importance of this set of thalamocortical connections in early cognitive development (Alcauter et al., 2013). This finding is consistent with the documented versatile functional roles of the salience network within different cognitive domains, including salience detection, emotion, working memory, explicit memory, and conflict monitoring (Smith et al., 2009; Menon and Uddin, 2010; Elton and Gao, 2014), all of which are critical skills essential for the overall intellectual growth of infants. Importantly, preliminary versions of these functions have been reported to experience significant improvements during the first years of life (Rothbart, 1990; Rothbart and Posner, 2001; Reznick, 2007; Tau and Peterson, 2010). Therefore, the versatile roles of the salience network that govern critical domains of early cognitive development may help explain its unique behavioral correlations during infancy.

Thalamus cluster connecting with the default mode network during infancy

The emergence of a thalamic cluster specifically projecting to the default mode network at 1 and 2 years of age is intriguing. As shown in Figure 3, it is clear that the identified default mode cluster projects to distributed default mode regions instead of localized areas, supporting the emergence of network-level thalamus–default network connectivity during infancy. The dramatic synchronization process of the default mode network during the first year of postnatal life (Gao et al., 2009b; Fig. 1) provides the network basis for the observed thalamus projection at this age. Moreover, animal tracing studies showed bidirectional connections between the posterior thalamic nucleus and the broad posterior cingulate/retrosplenial cortex in rhesus monkeys (Morris et al., 1999) and between the intralaminar nuclei and mPFC in rats (Berendse and Groenewegen, 1990, 1991; Ongür and Price, 2000), providing potential structural explanations for the observed connectivity. The location of the default mode thalamic cluster resembles the pulvinar nuclei (Niemann et al., 2000), which is consistent with its documented higher-order cortical projections observed in older populations (Behrens et al., 2003; Zhang et al., 2008; Fair et al., 2010; Zhang et al., 2010). Functionally, the default mode network is mainly involved in self-related mentation, although new evidence for other functions is emerging (Hampson et al., 2006; Gao and Lin, 2012; Gao et al., 2013a; Elton and Gao, 2014). Consistently, self-awareness and self-projection, lying at the core of default mode functions, have been observed to emerge ~1 year of age (Amsterdam, 1972; Herschkowitz, 2000). Therefore, the observed thalamus–default network connectivity could play a role in this self-concept-building process (Philippi et al., 2012). Overall, in addition to the salience network, the default network is the only other higher-order network that shows significant thalamus connectivity during infancy, which may reflect both the high importance of early self-concept construction and the critical roles of the thalamus in this process. Specific thalamocortical connectivity with other higher-order cortical networks (e.g., executive control) might develop at later ages, representing an interesting future direction.

Usage of cortical networks to define subthalamus clusters and other considerations

It is well known that the human brain cortex is organized into coherent and spatially distributed functional networks (Damoiseaux et al., 2006; Smith et al., 2009; Friston, 2011). Therefore, it makes sense to characterize thalamocortical functional connectivity based on cortical networks rather than on anatomically defined local regions. Consistent with this notion, our results showed well defined network-like connectivity profiles from all thalamic clusters. Therefore, although pending independent replication, we would suggest the use of functional networks as promising targets for delineating thalamocortical connectivity in future studies.

One potential concern might be that the thalamic parcellation results may be driven by the differential maturation status of different cortical functional networks. However, we used age-specific cortical network masks (Fig. 1) in the parcellation so the results should be relatively free from this maturation status bias. A second concern might be the adoption of a winner-takes-all approach. As noted previously, this approach could potentially mask secondary but significant connections. Therefore, retrospective examination of the projection patterns, as shown in Figure 3, is recommended. Finally, regarding motion artifacts, we have implemented the strategy combining the "scrubbing" process and residual FD regression (i.e., modeled as a covariate of no interest in all statistical analyses), which has been shown previously to produce robust results against motion artifacts (Gao et al., 2014b).

Conclusions

In conclusion, our results delineated the emergence of age-dependent thalamocortical connectivity patterns and their cognitive significance during infancy. Our results emphasized the early establishment of thalamus–primary network connectivity and highlighted the salience and default mode networks as the only higher-order networks showing specific thalamus connectivity during infancy. Further, the novel brain–behavior analyses revealed the unique importance of thalamus–salience network connectivity in early cognitive development. Given the close relationship between thalamocortical connectivity and various developmental brain disorders, the findings of this study provide a new perspective and reference for future delineation of abnormal functional connectivity in different developmental disorders.

References

Alcauter S, Lin W, Keith Smith J, Gilmore JH, Gao W (2013) Consistent anterior-posterior segregation of the insula during the first 2 years of life. Cereb Cortex, in press.

Amsterdam B (1972) Mirror self-image reactions before age two. Dev Psychobiol 5:297–305. CrossRef Medline

Anticevic A, Cole MW, Repovs G, Murray JD, Brumbaugh MS, Winkler AM, Savic A, Krystal JH, Pearlson GD, Glahn DC (2013) Characterizing thalamo-cortical disturbances in schizophrenia and bipolar illness. Cereb Cortex, in press.

Arichi T, Gordon-Williams R, Allievi A, Groves AM, Burdet E, Edwards AD (2013) Computer-controlled stimulation for functional magnetic resonance imaging studies of the neonatal olfactory system. Acta Paediatr 102:868–875. CrossRef Medline

Bartocci M, Bergqvist LL, Lagercrantz H, Anand KJ (2006) Pain activates cortical areas in the preterm newborn brain. Pain 122:109–117. CrossRef Medline

Behrens TE, Johansen-Berg H, Woolrich MW, Smith SM, Wheeler-Kingshott CA, Boulby PA, Barker GJ, Sillery EL, Sheehan K, Ciccarelli O, Thompson AJ, Brady JM, Matthews PM (2003) Non-invasive mapping of connections between human thalamus and cortex using diffusion imaging. Nat Neurosci 6:750–757. CrossRef Medline

Benjamini Y, Yekutieli D (2001) The control of the false discovery rate in multilpe testing under dependency. Annals of Statistics 29:1165–1188. CrossRef

Berendse HW, Groenewegen HJ (1990) Organization of the thalamostriatal projections in the rat, with special emphasis on the ventral striatum. J Comp Neurol 299:187–228. CrossRef Medline

Berendse HW, Groenewegen HJ (1991) Restricted cortical termination fields of the midline and intralaminar thalamic nuclei in the rat. Neuroscience 42:73–102. CrossRef Medline

Buckner RL, Krienen FM, Castellanos A, Diaz JC, Yeo BT (2011) The organization of the human cerebellum estimated by intrinsic functional connectivity. J Neurophysiol 106:2322–2345. CrossRef Medline

Cheatham CL, Goldman BD, Fischer LM, da Costa KA, Reznick JS, Zeisel SH (2012) Phosphatidylcholine supplementation in pregnant women consuming moderate-choline diets does not enhance infant cognitive function: a randomized, double-blind, placebo-controlled trial. Am J Clin Nutr 96:1465–1472. CrossRef Medline

Damoiseaux JS, Rombouts SA, Barkhof F, Scheltens P, Stam CJ, Smith SM, Beckmann CF (2006) Consistent resting-state networks across healthy subjects. Proc Natl Acad Sci U S A 103:13848–13853. CrossRef Medline

Desikan RS, Ségonne F, Fischl B, Quinn BT, Dickerson BC, Blacker D, Buckner RL, Dale AM, Maguire RP, Hyman BT, Albert MS, Killiany RJ (2006) An automated labeling system for subdividing the human cerebral cortex on MRI scans into gyral based regions of interest. Neuroimage 31:968–980. CrossRef Medline

Doria V, Beckmann CF, Arichi T, Merchant N, Groppo M, Turkheimer FE, Counsell SJ, Murgasova M, Aljabar P, Nunes RG, Larkman DJ, Rees G, Edwards AD (2010) Emergence of resting state networks in the preterm human brain. Proc Natl Acad Sci U S A 107:20015–20020. CrossRef Medline

Elton A, Gao W (2014) Divergent task-dependent functional connectivity of executive control and salience networks. Cortex 51:56–66. CrossRef Medline

Fair DA, Bathula D, Mills KL, Dias TG, Blythe MS, Zhang D, Snyder AZ, Raichle ME, Stevens AA, Nigg JT, Nagel BJ (2010) Maturing thalamocortical functional connectivity across development. Front Syst Neurosci 4:10. CrossRef Medline

Fransson P, Skiöld B, Horsch S, Nordell A, Blennow M, Lagercrantz H, Aden U (2007) Resting-state networks in the infant brain. Proc Natl Acad Sci U S A 104:15531–15536. CrossRef Medline

Frazier JA, Chiu S, Breeze JL, Makris N, Lange N, Kennedy DN, Herbert MR, Bent EK, Koneru VK, Dieterich ME, Hodge SM, Rauch SL, Grant PE, Cohen BM, Seidman LJ, Caviness VS, Biederman J (2005) Structural brain magnetic resonance imaging of limbic and thalamic volumes in pediatric bipolar disorder. Am J Psychiatry 162:1256–1265. CrossRef Medline

Friston KJ (2011) Functional and effective connectivity: a review. Brain Connect 1:13–36. CrossRef Medline

Gao W, Lin W (2012) Frontal parietal control network regulates the anti-correlated default and dorsal attention networks. Hum Brain Mapp 33:192–202. CrossRef Medline

Gao W, Lin W, Chen Y, Gerig G, Smith JK, Jewells V, Gilmore JH (2009a) Temporal and spatial development of axonal maturation and myelination of white matter in the developing brain. AJNR Am J Neuroradiol 30:290–296. CrossRef Medline

Gao W, Zhu H, Giovanello KS, Smith JK, Shen D, Gilmore JH, Lin W (2009b) Evidence on the emergence of the brain's default network from 2-week-old to 2-year-old healthy pediatric subjects. Proc Natl Acad Sci U S A 106:6790–6795. CrossRef Medline

Gao W, Gilmore JH, Giovanello KS, Smith JK, Shen D, Zhu H, Lin W (2011) Temporal and spatial evolution of brain network topology during the first two years of life. PLoS One 6:e25278. CrossRef Medline

Gao W, Gilmore JH, Alcauter S, Lin W (2013a) The dynamic reorganization of the default-mode network during a visual classification task. Front Syst Neurosci 7:34. CrossRef Medline

Gao W, Gilmore JH, Shen D, Smith JK, Zhu H, Lin W (2013b) The synchronization within and interaction between the default and dorsal attention networks in early infancy. Cereb Cortex 23:594–603. CrossRef Medline

Gao W, Alcauter S, Elton A, Hernandez-Castillo CR, Smith JK, Ramirez J, Lin W (2014a) Functional network development during the first year: relative sequence and socioeconomic correlations. Cereb Cortex, in press.

Gao W, Alcauter S, Smith JK, Gilmore JH, Lin W (2014b) Development of human brain cortical network architecture during infancy. Brain Struct Funct, in press.

Gilmore JH, Lin W, Prastawa MW, Looney CB, Vetsa YS, Knickmeyer RC, Evans DD, Smith JK, Hamer RM, Lieberman JA, Gerig G (2007) Regional gray matter growth, sexual dimorphism, and cerebral asymmetry in the neonatal brain. J Neurosci 27:1255–1260. CrossRef Medline

Gilmore JH, Shi F, Woolson SL, Knickmeyer RC, Short SJ, Lin W, Zhu H,

Hamer RM, Styner M, Shen D (2012) Longitudinal development of cortical and subcortical gray matter from birth to 2 years. Cereb Cortex 22:2478–2485. CrossRef Medline

Guldenmund P, Demertzi A, Boveroux P, Boly M, Vanhaudenhuyse A, Bruno MA, Gosseries O, Noirhomme Q, Brichant JF, Bonhomme V, Laureys S, Soddu A (2013) Thalamus, brainstem and salience network connectivity changes during propofol-induced sedation and unconsciousness. Brain Connect 3:273–285. CrossRef Medline

Hampson M, Driesen NR, Skudlarski P, Gore JC, Constable RT (2006) Brain connectivity related to working memory performance. J Neurosci 26:13338–13343. CrossRef Medline

Herschkowitz N (2000) Neurological bases of behavioral development in infancy. Brain Dev 22:411–416. CrossRef Medline

Iacoboni M, Woods RP, Brass M, Bekkering H, Mazziotta JC, Rizzolatti G (1999) Cortical mechanisms of human imitation. Science 286:2526–2528. CrossRef Medline

Jenkinson M, Beckmann CF, Behrens TE, Woolrich MW, Smith SM (2012) FSL. Neuroimage 62:782–790. CrossRef Medline

Jones EG (2007) The thalamus, Ed 2. Cambridge: Cambridge University.

Kim DJ, Park B, Park HJ (2013) Functional connectivity-based identification of subdivisions of the basal ganglia and thalamus using multilevel independent component analysis of resting state fMRI. Hum Brain Mapp 34:1371–1385. CrossRef Medline

Klingner CM, Langbein K, Dietzek M, Smesny S, Witte OW, Sauer H, Nenadic I (2014) Thalamocortical connectivity during resting state in schizophrenia. Eur Arch Psychiatry Clin Neurosci 264:111–119. CrossRef Medline

Knickmeyer RC, Gouttard S, Kang C, Evans D, Wilber K, Smith JK, Hamer RM, Lin W, Gerig G, Gilmore JH (2008) A structural MRI study of human brain development from birth to 2 years. J Neurosci 28:12176–12182. CrossRef Medline

Kostovic I, Goldman-Rakic PS (1983) Transient cholinesterase staining in the mediodorsal nucleus of the thalamus and its connections in the developing human and monkey brain. J Comp Neurol 219:431–447. Medline

Kostovic I, Rakic P (1984) Development of prestriate visual projections in the monkey and human fetal cerebrum revealed by transient cholinesterase staining. J Neurosci 4: 25–42. Medline

Lin W, Zhu Q, Gao W, Chen Y, Toh CH, Styner M, Gerig G, Smith JK, Biswal B, Gilmore JH (2008) Functional connectivity MR imaging reveals cortical functional connectivity in the developing brain. AJNR Am J Neuroradiol 29:1883–1889. CrossRef Medline

Luo L, O'Leary DD (2005) Axon retraction and degeneration in development and disease. Annu Rev Neurosci 28:127–156. CrossRef Medline

Marenco S, Stein JL, Savostyanova AA, Sambataro F, Tan HY, Goldman AL, Verchinski BA, Barnett AS, Dickinson D, Apud JA, Callicott JH, Meyer-Lindenberg A, Weinberger DR (2012) Investigation of anatomical thalamo-cortical connectivity and FMRI activation in schizophrenia. Neuropsychopharmacology 37:499–507. CrossRef Medline

Menon V, Uddin LQ (2010) Saliency, switching, attention and control: a network model of insula function. Brain Struct Funct 214:655–667. CrossRef Medline

Morris R, Petrides M, Pandya DN (1999) Architecture and connections of retrosplenial area 30 in the rhesus monkey (*Macaca mulatta*). Eur J Neurosci 11:2506–2518. CrossRef Medline

Mullen EM (1995) Mullen scales of early learning manual, AGS edition. Circle Pines, MN: American Guidance Service.

Nair A, Treiber JM, Shukla DK, Shih P, Müller RA (2013) Impaired thalamocortical connectivity in autism spectrum disorder: a study of functional and anatomical connectivity. Brain 136:1942–1955. CrossRef Medline

Niemann K, Mennicken VR, Jeanmonod D, Morel A (2000) The Morel stereotactic atlas of the human thalamus: atlas-to-MR registration of internally consistent canonical model. Neuroimage 12:601–616. CrossRef Medline

O'Leary DD, Koester SE (1993) Development of projection neuron types, axon pathways, and patterned connections of the mammalian cortex. Neuron 10:991–1006. CrossRef Medline

Ongür D, Price JL (2000) The organization of networks within the orbital and medial prefrontal cortex of rats, monkeys and humans. Cereb Cortex 10:206–219. CrossRef Medline

Pelphrey KA, Reznick JS (2003) Working memory in infancy. Adv Child Dev Behav 31:173–227. Medline

Pelphrey KA, Reznick JS, Davis Goldman B, Sasson N, Morrow J, Donahoe A, Hodgson K (2004) Development of visuospatial short-term memory in the second half of the 1st year. Dev Psychol 40:836–851. CrossRef Medline

Philippi CL, Feinstein JS, Khalsa SS, Damasio A, Tranel D, Landini G, Williford K, Rudrauf D (2012) Preserved self-awareness following extensive bilateral brain damage to the insula, anterior cingulate, and medial prefrontal cortices. PLoS One 7:e38413. CrossRef Medline

Porter RH, Winberg J (1999) Unique salience of maternal breast odors for newborn infants. Neurosci Biobehav Rev 23:439–449. CrossRef Medline

Power JD, Barnes KA, Snyder AZ, Schlaggar BL, Petersen SE (2012) Spurious but systematic correlations in functional connectivity MRI networks arise from subject motion. Neuroimage 59:2142–2154. CrossRef Medline

Rakic P, Goldman-Rakic PS (1982) The development and modifiability of the cerebral cortex. Overview. Neurosci Res Program Bull 20:433–438. Medline

Reznick JS (2007) Working memory in infants and toddlers. In: Short-and long-term memory in infancy and early childhood: taking the first steps toward remembering (Oakes LM, Bauer PJ, eds), pp 3–26. Oxford: OUP.

Reznick JS (2009) Working memory in infants and toddlers. In: The development of memory in infancy and childhood, Ed 2, pp xii. New York: Psychology.

Reznick JS, Morrow JD, Goldman BD, Snyder J (2004) The onset of working memory in infants. Infancy 6:145–154. CrossRef

Rothbart MK (1990) Regulatory mechanisms in infant development. Amsterdam: Elsevier/North-Holland.

Rothbart MK, Posner MI (2001) Mechanism and variation in the development of attentional networks. Cambridge: MIT.

Seeley WW, Menon V, Schatzberg AF, Keller J, Glover GH, Kenna H, Reiss AL, Greicius MD (2007) Dissociable intrinsic connectivity networks for salience processing and executive control. J Neurosci 27:2349–2356. CrossRef Medline

Sharma J, Angelucci A, Sur M (2000) Induction of visual orientation modules in auditory cortex. Nature 404:841–847. CrossRef Medline

Shen D, Davatzikos C (2004) Measuring temporal morphological changes robustly in brain MR images via 4-dimensional template warping. Neuroimage 21:1508–1517. CrossRef Medline

Sherman SM (2007) The thalamus is more than just a relay. Curr Opin Neurobiol 17:417–422. CrossRef Medline

Shibata M, Fuchino Y, Naoi N, Kohno S, Kawai M, Okanoya K, Myowa-Yamakoshi M (2012) Broad cortical activation in response to tactile stimulation in newborns. Neuroreport 23:373–377. CrossRef Medline

Short SJ, Elison JT, Goldman BD, Styner M, Gu H, Connelly M, Maltbie E, Woolson S, Lin W, Gerig G, Reznick JS, Gilmore JH (2013) Associations between white matter microstructure and infants' working memory. Neuroimage 64:156–166. CrossRef Medline

Smith SM, Jenkinson M, Woolrich MW, Beckmann CF, Behrens TE, Johansen-Berg H, Bannister PR, De Luca M, Drobnjak I, Flitney DE, Niazy RK, Saunders J, Vickers J, Zhang Y, De Stefano N, Brady JM, Matthews PM (2004) Advances in functional and structural MR image analysis and implementation as FSL. Neuroimage 23:S208–S219. CrossRef Medline

Smith SM, Fox PT, Miller KL, Glahn DC, Fox PM, Mackay CE, Filippini N, Watkins KE, Toro R, Laird AR, Beckmann CF (2009) Correspondence of the brain's functional architecture during activation and rest. Proc Natl Acad Sci U S A 106:13040–13045. CrossRef Medline

Stanfield BB, O'Leary DD, Fricks C (1982) Selective collateral elimination in early postnatal development restricts cortical distribution of rat pyramidal tract neurones. Nature 298:371–373. CrossRef Medline

Tau GZ, Peterson BS (2010) Normal development of brain circuits. Neuropsychopharmacology 35:147–168. CrossRef Medline

Varendi H, Porter RH (2001) Breast odour as the only maternal stimulus elicits crawling towards the odour source. Acta Paediatr 90:372–375. CrossRef Medline

Verbeke G, Molenberghs G (2009) Linear mixed models for longitudinal data. New York: Springer.

Yeo BT, Krienen FM, Sepulcre J, Sabuncu MR, Lashkari D, Hollinshead M, Roffman JL, Smoller JW, Zöllei L, Polimeni JR, Fischl B, Liu H, Buckner RL (2011) The organization of the human cerebral cortex estimated by intrinsic functional connectivity. J Neurophysiol 106:1125–1165. CrossRef Medline

Zhang D, Snyder AZ, Fox MD, Sansbury MW, Shimony JS, Raichle ME (2008) Intrinsic functional relations between human cerebral cortex and thalamus. J Neurophysiol 100:1740–1748. CrossRef Medline

Zhang D, Snyder AZ, Shimony JS, Fox MD, Raichle ME (2010) Noninvasive functional and structural connectivity mapping of the human thalamocortical system. Cereb Cortex 20:1187–1194. CrossRef Medline